Coronin 7, the mammalian POD-1 homologue, localizes to the Golgi apparatus

Vasily Rybakin[a], Maria Stumpf[a], Andrea Schulze[a], Irina V. Majoul[b], Angelika A. Noegel[a,*], Andreas Hasse[a]

[a] *Center for Biochemistry, Institute of Biochemistry I, Medical Faculty, University of Cologne, Joseph-Stelzmann-Str. 52, D-50931 Cologne, Germany*
[b] *University of Cambridge, Cambridge Institute for Medical Research, Addenbrooke's Hospital Site, Hills Road, Cambridge CB2 2XY, UK*

Received 21 May 2004; revised 21 July 2004; accepted 26 July 2004

Available online 9 August 2004

Edited by Felix Wieland

Abstract Coronins constitute an evolutionary conserved family of WD-repeat actin-binding proteins. Their primary function is thought to be regulating the actin cytoskeleton. Apart from that, several coronins were indirectly shown to participate in vesicular transport, establishment of cell polarity and cytokinesis. Here, we report a novel mammalian protein, coronin 7 (crn7), which is significantly different from other mammalian coronins in its domain architecture. Crn7 possesses two stretches of WD repeats in contrast to the other coronins only having one. The protein is expressed throughout the mouse embryogenesis and is strongly upregulated in brain and developing structures of the immune system in the course of development. In adult animals, both crn7 mRNA and protein are abundantly present in most organs, with significantly higher amounts in brain, kidney, thymus and spleen and lower amounts in muscle. At the subcellular level, the bulk of the protein appears to be present in the cytosol and in large cytosolic complexes. However, a significant portion of the protein is detected on vesicle-like cytoplasmic structures as well as on the *cis*-Golgi. In the Golgi region, crn7 staining appears broader than that of the *cis*-Golgi markers Erd2p and β-COP, still, the *trans*-Golgi network appears predominantly crn7-negative. Importantly, the membrane-associated form of crn7 protein is phosphorylated on tyrosine residues, whereas the cytosolic form is not. Crn7 is the first coronin protein proven to localize to the Golgi membrane. We conclude that it plays a role in the organization of intracellular membrane compartments and vesicular trafficking rather than in remodeling the cytoskeleton.

Keywords: Cytoskeleton; Vesicular trafficking; Golgi apparatus; Brain development; Phosphorylation; WD repeats

1. Introduction

Coronins are a family of evolutionary conserved actin-binding proteins found in a variety of organisms from *Dictyostelium* to man. A common structural feature of the approx. 55 kDa coronin proteins is the presence of a conserved central stretch of WD-40 domain repeats that are proposed to form a propeller-like structure [1] and a C-terminal coiled coil region. The first family member was characterized in *Dictyostelium* and was shown to mediate actin cytoskeleton remodeling and phagocytosis [2–4]. In addition to this role, the other members have been shown to function in vesicular trafficking, cell division and establishment of cell polarity, although none of these functions is completely abolished in coronin-mutant cells (reviewed in [1]). The coiled coil regions of coronin proteins participate in their homophilic di- and oligomerization [5,6], whereas the WD-repeats are implied in actin binding [7,8]. In the yeast, the coronin orthologue crn1p associates with the Arp2/3 complex and inhibits actin nucleation in vitro, the inhibitory function being mapped to the coiled coil region [9]. The yeast coronin has also been shown to interact with the microtubule cytoskeleton in an actin-dependent manner [7,10].

In mammals, most coronin-related genes are expressed in a tissue-specific manner, only coronins 2 and 3 being ubiquitous. Isoforms 4 and 5 are expressed in the brain, coronin 2_{SE} in epithelial tissues and coronin 1 in the hematopoietic lineage and in the lung (reviewed in [1]). Not much data are available on the functions of mammalian coronins. It was shown that the isoform 1 ($p57^{crn1}$) is localized to phagosomes and is released upon PKC-dependent phosphorylation [11]. GST-fused recombinant coronin 1 binds actin in vitro [12]. Surprisingly, actin binding was later conferred not only to the WD repeats, but also to the short N-terminal region of the protein [8].

Two recently discovered *Drosophila* and *C. elegans* proteins seem to constitute a novel subfamily of coronins. The worm POD-1 and fly Dpod-1 are both approximately twice as long as conventional coronins (predicted molecular weight of 115 and 119 kDa, respectively) and possess two stretches of WD repeats each, but no coiled coil region. As both N- and C-termini of POD-1 proteins possess a significant degree of homology to the conventional coronins, it might be presumed that the corresponding genes have arisen due to gene duplication. *C. elegans* POD-1 has been shown to participate in polar granule trafficking and thus in polarization of the early embryo [13]. POD-1 mutant embryos also accumulate abnormal membranous structures in the cytoplasm and show a defect in the formation of secreted extracellular structures (eggshell), resulting in an increase in osmotic sensitivity and permeability of dyes. Dpod1, the *Drosophila* homologue, plays a role in the axonal growth cone targeting and cross-links both actin and microtubules [14]. In addition to the WD-40 domains, the *Drosophila*

* Corresponding author. Fax: +49-221-478-6979.
E-mail address: noegel@uni-koeln.de (A.A. Noegel).

0014-5793/$22.00
doi:10.1016/j.febslet.2004.07.066

protein possesses a predicted microtubule-binding domain similar to that of the microtubule-binding protein MAP1B.

Here, we report a novel mammalian coronin similar to both POD-1 proteins. Although being considerably shorter, it possesses the same molecular architecture as the worm POD-1 and lacks the MAP-like domain of the Dpod-1. Using a current nomenclature [15], we named it coronin 7 (crn7). We show that the protein is ubiquitously distributed in most human and mouse cells and tissues throughout development. Its subcellular localization suggests a role in Golgi-related vesicular trafficking events.

2. Materials and methods

2.1. Molecular cloning, sequence analysis

A complete human crn7 ORF was contained in the HEPG2 cDNA clone HEP08253 (Accession No. AK025674, obtained from the MRC Centre, Cambridge, UK). The sequence was verified and inserted in frame into pEGFP-C1 plasmid (Clontech). Plasmid DNA used for transfection was prepared and purified using Nucleobond AX plasmid midi or maxi kits (Macherey and Nagel). We used the GeneBee server (Moscow State University, Russia) for phylogenetic analysis of the coronin family members, and ClustalW (EBI, UK) and BLAST (NCBI) for sequence alignments.

2.2. Generation of a monoclonal antibody

A 500 bp fragment coding for the C-terminal 160 amino acids of human crn7 was inserted into pQE30 plasmid (Qiagen) for expression as a 6× His-tagged polypeptide. Expression in *Escherichia coli* M15 [pREP4] was induced with 0.5 mM IPTG. Purification of the His-tagged protein by nickel nitrilotriacetate (Ni-NTA) agarose (Qiagen) affinity chromatography was performed according to the manufacturer's instructions. Immunization of female Balb/c mice was done using the Immuneasy kit (Qiagen). Antibodies were generated according to standard protocols. The monoclonal antibody derived from the clone K37-142-1 was used for detection of crn7 protein in all the experiments described.

2.3. Mammalian Cell Culture

NIH 3T3 cells were grown in a Dulbecco's modified Eagle's medium containing 4.5 g/L glucose (Sigma), supplemented with 10% fetal calf serum (Biochrom), 2 mM L-glutamine (Biochrom), 1 mM sodium pyruvate (Biochrom), 100 units/ml penicillin G, and 100 μg/ml streptomycin (Invitrogen). For immunostaining, the cells were grown on 12 mm glass coverslips. For drug studies, the following substances were added to the serum-free culture medium: latrunculin B (Sigma) at 1 μg/ml for 30 min, brefeldin A (Fluka) at 20 μg/ml for 5 min, colchicine (Fluka) at 5 μg/ml for 30 min, nocodazole (Sigma) at 33 μM for 30 min.

2.4. Antibodies and immunoblotting

Protein samples were separated by SDS–PAGE (10% acrylamide) and blotted onto nitrocellulose filters. Unspecific binding of the antibodies was blocked with 4% skimmed milk and 1% BSA in TBS-T (10 mM Tris–HCl, pH 8.0, 150 mM NaCl, and 0.2% Tween 20). The following primary antibodies were used: monoclonal anti-crn7 K37-142-1, β-actin specific mAb AC74 (Sigma) at 1:10 000, rabbit polyclonal anti-Rab5 (Transduction Laboratories) at 1:250, anti-phosphotyrosine mAb at 1:50, rabbit anti-phosphoserine/phosphothreonine at 1:1000. Horseradish peroxidase-conjugated secondary antibodies against murine and rabbit IgG (Pierce) were used at 1:7500 and 1:10 000, respectively.

2.5. Immunostaining and imaging

The cells were washed briefly with PBS, fixed with 4% paraformaldehyde at room temperature, rinsed with 20 mM glycine and permeabilized with 0.2% saponin in PBS. Saponin was present in the buffers at all later stages of staining at the concentration of 0.02%. Unspecific binding of the antibodies was blocked with 0.045% fish gelatin and 0.5% BSA, in PBS. The following primary antibodies were used: anti-crn7 mAb K37-142-1 at 1:75, anti-Erd2p polyclonal antibody [16] at 1:50, polyclonal anti-TGN38 (provided by Dr. Mark McNiven) at 1:150, polyclonal anti-LIMP1 (provided by Dr. Yoshitaka Tanaka) at 1:50, and polyclonal anti-β-COP at 1:50. Secondary goat anti-mouse antibody conjugated with Cy3 (Sigma) was used at 1:2000 and sheep anti-rabbit antibody conjugated with FITC (BioRad) at 1:1000. Coverslips were mounted in gelvatol and analyzed using a Leica fluorescent microscope as described [6]. Digital images were acquired using SensiControl 4.03 software (PCO Computer Optics, Germany). Immunohistochemical analysis was performed on paraffin-embedded 5-μm sections of paraformaldehyde-fixed murine tissues. The deparaffinized sections were treated with a 1:75 dilution of affinity purified anti-crn7 antibody overnight at 4 °C and a 1:500 dilution of Alexa 488-conjugated anti-IgG1 secondary antibody (Molecular Probes) for 2 h at room temperature. Sections were counterstained with DAPI and visualized by fluorescence microscopy.

2.6. Subcellular fractionation and two-dimensional gel electrophoresis

Subcellular fractionation experiments were performed as described [6], except for cell homogenization which was performed by passing the cells through a 21G $1\frac{1}{2}$ needle for 15 times. For phosphorylation assays, all the steps were performed in the presence of 1 mM sodium orthovanadate and 25 nM okadaic acid (BioChemika). Separation of membrane organelles on discontinuous sucrose gradients and two-dimensional gel electrophoresis were performed as described [6].

3. Results

3.1. Crn7 is a mammalian POD-1 protein

We have cloned a complete cDNA for human crn7 by reverse-transcriptase PCR using information from the EST database. The obtained sequence contains a single open reading frame encoding a 924-amino acid protein (Fig. 1) with a predicted molecular weight of 100.5 kDa and a predicted isoelectric point of 5.6. The predicted protein sequence contains two coronin domains, as the related *C. elegans* POD-1 and dPOD-1 from *Drosophila* do. A structural peculiarity of crn7 is the presence of a 47-amino acid long proline, serine and threonine-enriched stretch preceding the second group of WD repeats designated a PST motif (Fig. 1). Crn7 protein is 46% and 47% homologous and 30% and 29% identical to Dpod-1 and POD-1, respectively as predicted by NCBI BLAST server using BLOSUM62 matrix. Using the information available from the *Dictyostelium discoideum* genome project, we also identified a closely related predicted protein in *Dictyostelium*. DdPOD-1 is a 962 amino acid protein 50% homologous and 29% identical to crn7 and possessing the same molecular architecture, including a PST motif. Phylogenetic analysis using cluster algorithm clearly positions crn7, ddPOD-1 and both previously described POD-1 proteins in a group distinct from other coronins (Fig. 2).

3.2. Tissue distribution and developmental dynamics of crn7

We have studied the localization of crn7 protein and mRNA in cells and tissues using our monoclonal antibody mAb K37-142-1 generated against a C-terminal polypeptide for Western blot and a full-length cDNA for Northern blot analysis. As indicated by Northern blots, the approximately 4 kb crn7 mRNA is present in the mouse embryonic tissues as early as at the day 5 p.c., and is significantly elevated to the day 15 (data not shown). Crn7 mRNA is expressed in the majority of mouse tissues, except for the lung, with a strong increase in brain, thymus and kidney (Fig. 3A). This pattern roughly corresponds to that of crn7 protein recognized by mAb K37-142-1 at approx. 100 kDa. The protein levels are comparatively low in both skeletal and heart muscle (Fig. 3B). The discrepancy

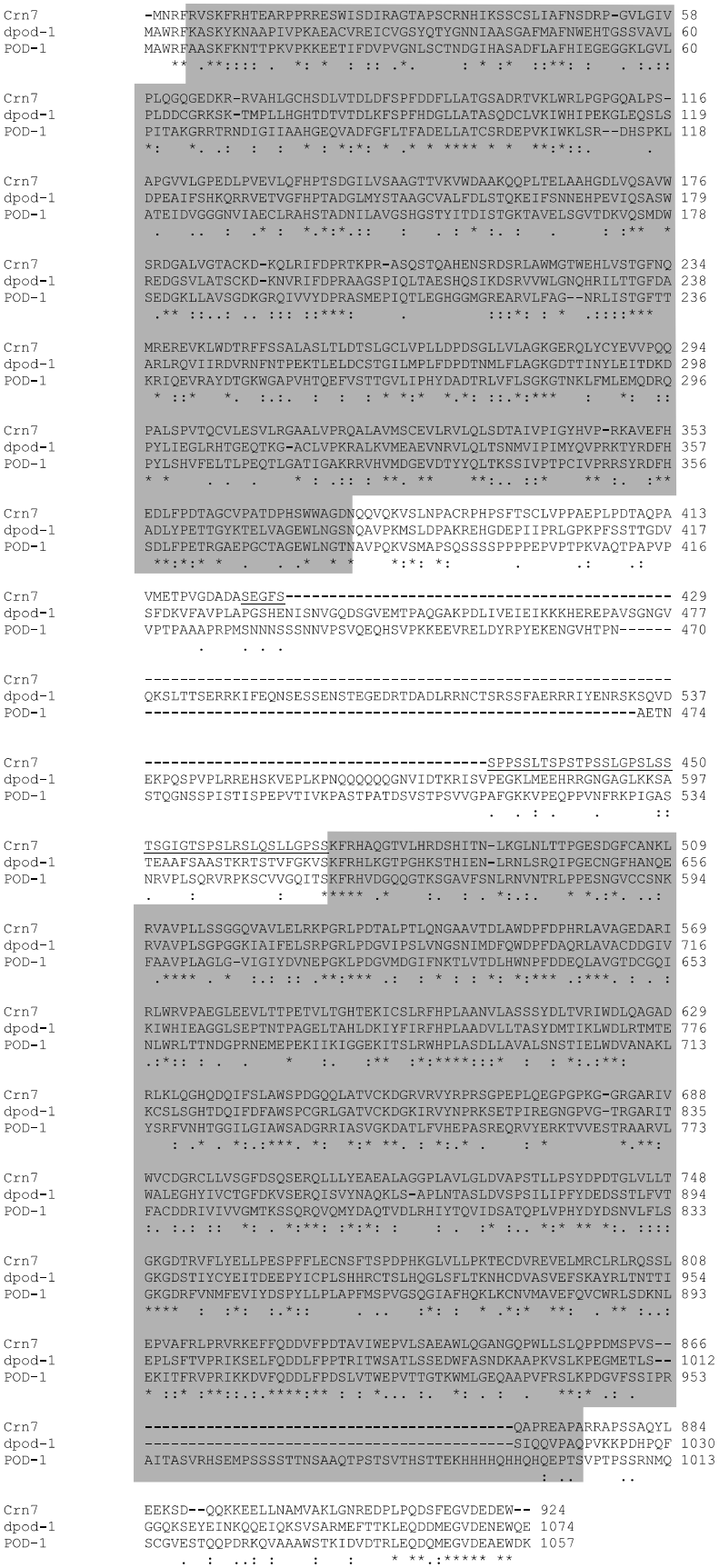

Fig. 1. Sequence alignment of human crn7 protein with POD-1 proteins from *Drosophila* and *C. elegans*. The coronin domains are highlighted in gray, the serine-, proline-, threonine-enriched sequence of crn7 is underlined.

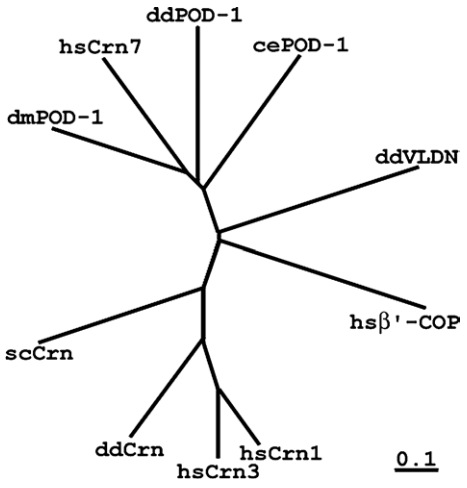

Fig. 2. Phylogenetic analysis of the coronin family members, including POD-1 proteins, performed using the cluster algorithm. dmPOD-1, *Drosophila* dPOD-1 protein; cePOD1, *C. elegans* POD-1; ddPOD-1, predicted POD-1 protein from *Dictyostelium*; hsCrn1, 3, 7, human coronins 1, 3 and 7, respectively; ddCrn, *Dictyostelium* coronin; scCrn, yeast (*Saccharomyces cerevisiae*) coronin; ddVLDN, *Dictyostelium* villidin; hsβ′-COP, human β′-COP. Multiple WD-repeat proteins villidin and β′-COP are clearly forming outgroups with regard to both coronins and POD-1 proteins. The bar corresponds to 10% of amino acid substitution within the branch.

between the mRNA and protein levels in certain tissues may indicate the presence of translational regulation of crn7. Using indirect immunofluorescence, we studied the developmental expression of the protein. The strongest expression is found in the embryonic brain, thymus, intestine, skin and in the eye. In the brain cortex, the crn7 protein is restricted to the most apical cell layers before embryonic day 10 (Fig. 4A and B) and shifted to a population of more basal cells thereafter (Fig. 4C and D), whereas in the hypothalamus the protein is detected in the same set of profound big neurons throughout development (Fig. 4E–G). In addition, the protein is found in the bodies and dendrites of Purkinje cells in the cerebellum (Fig. 4H). In the skin, crn7 is only present in the apical epidermis layers (Fig. 4I). The differentiating cells in the embryonic eye are also found to be crn7 positive (Fig. 4K). Here, crn7 is found in developing lens fibers. In adult mice, the protein is strongly expressed in the outer plexiform layer of the retina, where the rods are located (data not shown). Interestingly, in the intestine, the protein is found not only in terminally differentiated epithelial cells, but also in the crypt epithelium where the stem cells are located (Fig. 4J).

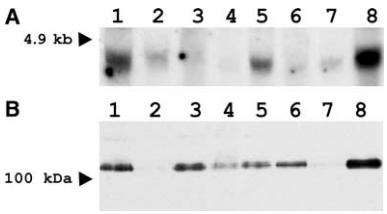

Fig. 3. Tissue distribution of the crn7 mRNA and protein. (A) total RNA from selected murine tissues was hybridized with the radioactively labeled crn7-specific probe. 1, brain; 2, heart; 3, liver; 4, lung; 5, kidney; 6, testis; 7, muscle; 8, thymus. (B) tissue lysates were separated on 10% SDS–polyacrylamide gels, blotted onto a nitrocellulose filter and probed with monoclonal anti-crn7 antibody K37-142-1. Lane description as in (A). Anti-β-actin monoclonal antibody was used to confirm equal loading (data not shown).

3.3. Subcellular localization of crn7

Using indirect immunofluorescence, we analyzed the cellular distribution of crn7. The protein is found in vesicle-like structures and in a Golgi-like perinuclear compartment (Fig. 5). The crn7-positive perinuclear structure is most prominent in NIH 3T3 fibroblasts, although most other

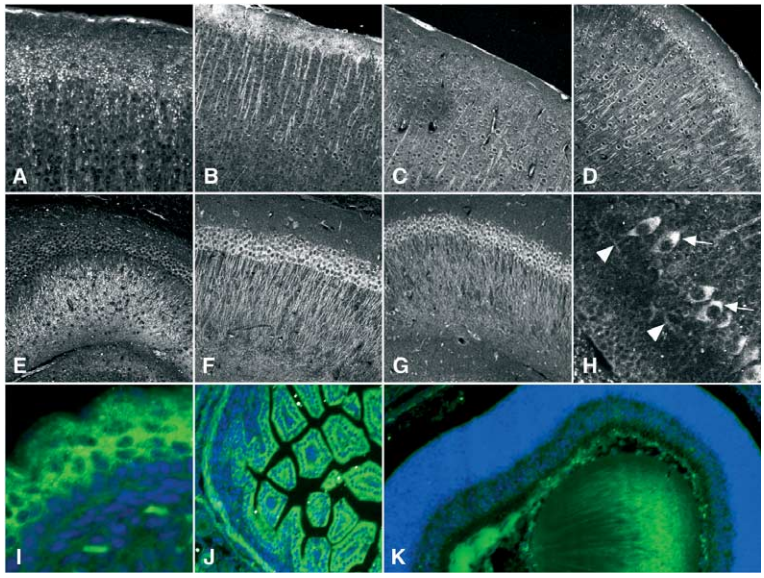

Fig. 4. Immunolocalization of the crn7 protein in paraformaldehyde-fixed murine embryonic tissues. (A)–(D) Sections through the brain cortex at the embryonic days 5, 10, 20 and 30, respectively. (E)–(G) Section through the hippocampus at the embryonic days 10, 20 and 30, respectively. (H) Localization of the crn7 protein in the Purkinje cell bodies (arrows) and dendrites (arrowheads). (I)–(K) Embryonic skin, intestine and lens, respectively, at the day 16 of development. Top of the images A–G and I correspond to the apical side of the corresponding organs. Immunostaining was performed using monoclonal anti-crn7 antibody K37-142-1 (green in I–K). Primary antibodies were detected by Alexa 488-conjugated anti-IgG1 secondary antibody. Sections were counter-stained with DAPI (blue in I–K).

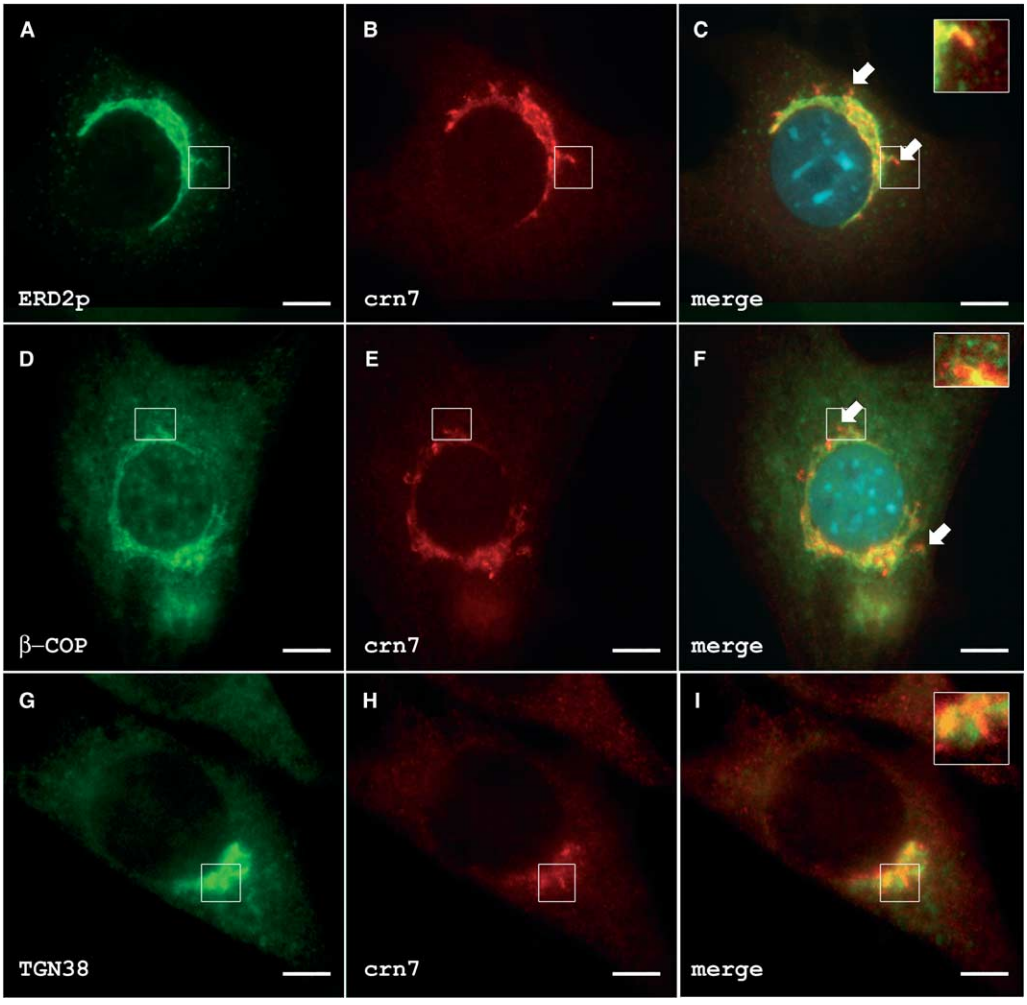

Fig. 5. Immunolocalization of the crn7 protein in NIH 3T3 cells. Paraformaldehyde-fixed cells were stained with monoclonal anti-crn7 antibody K37-142-1 (B, E, H) and rabbit polyclonal antibodies against either Erd2p (A), β-COP (D), or TGN38 (G). Primary antibodies were detected with goat anti-mouse antibody conjugated with Cy3 (red) and sheep anti-rabbit antibody conjugated with FITC (green). (C), (F), (I) Merged false color images. Insets in C, F, I correspond to the areas marked in A–C, D–F and G–I, respectively. Bar, 10 μm.

studied cell types show a similar pattern of distribution (data not shown). Crn7 protein co-localizes with *cis*-Golgi markers β-COP and Erd2p in the Golgi region as shown by indirect immunofluorescence (Fig. 5). It is noteworthy that (a) in both cases the crn7 antibody stains a broader *trans*-Golgi region than do both Golgi marker antibodies (Fig. 5C and F, arrows), and (b) the cytosolic crn7-positive vesicles are clearly distinct from the Erd2p- or β-COP-positive ones. *cis*-Golgi localization of crn7 was further confirmed by immunostaining NIH 3T3 fibroblasts expressing GFP-fused *cis*-Golgi markers p23 and GM130 with crn7 antibody (data not shown). Importantly, although we were able to observe a certain co-localization of crn7 with the *trans*-Golgi marker TGN38, such co-localization was restricted to the proximal Golgi region and almost absent in the *trans*-most cisternae (Fig. 5I).

Upon treatment with brefeldin A, an agent leading to the disruption of the Golgi and its fusion with the ER, the perinuclear crn7-labeled structure disappears and crn7-staining occurs in dots (Fig. 6A–C). As a control for this experiment, we used the Erd2-specific polyclonal antibody [16] which showed a similar staining pattern and still partially co-localized with crn7 after BFA treatment. Upon treatment with 5 μg/ml colchicine for 30 min, the perinuclear crn7- and the Erd2-positive compartment disassemble, both markers staying partially co-localized (Fig. 6D–F). The same result was obtained by using nocodazole at 33 μM for 30 min (data not shown). A similar disassembly of the crn7-labelled structure is also observed in mitotic cells (data not shown). In spite of our data indicating the influence of microtubule-disrupting agents on the architecture of the crn7-positive Golgi compartment and the observation that this compartment partially co-localizes with microtubules (data not shown), we assume that such co-localization reflects the ability of the corresponding membrane structures to bind to the microtubule network [17] rather than indicating a direct binding of the crn7 protein to tubulin as crn7 lacks any known MT-interacting motifs. We did not observe any co-localization of the cytosolic crn7 structures with actin filaments (data not shown).

The cytoplasmic crn7-labeled structures (Fig. 5) do not correspond to the intermediates of the endocytic pathway, as they do not co-localize with transferrin-positive compartments after 1, 5, 10, 30 or 60 min of the internalization of FITC-

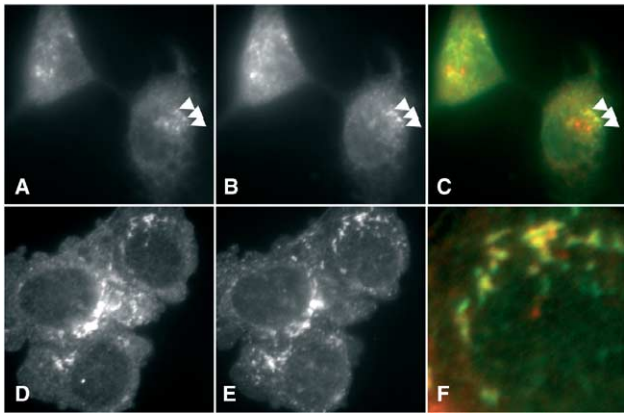

Fig. 6. Influence of brefeldin A and colchicine on cellular distribution of crn7. (A)–(C) Cells treated with 20 μg/ml brefeldin A for 5 min. (D)–(F) Cells treated with 5 μg/ml colchicine for 30 min. (J), (I) Anti-crn7 antibody. (B), (E) Anti-Erd2p antiserum. (C), (F) Merged false color images (colors as in Fig. 5).

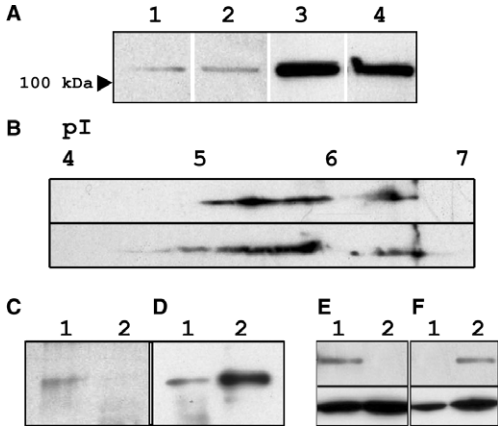

Fig. 7. (A) Differential centrifugation experiment showing the presence of the crn7 protein in heavy membrane/cytoskeletal fraction ($10\,000 \times g$ pellet, lane 1), light membrane fraction ($100\,000 \times g$ pellet, lane 2), cytosolic protein complexes ($200\,000 \times g$ pellet, lane 3) and cytosol ($200\,000 \times g$ supernatant, lane 4) of NIH 3T3 cells. (B) Two-dimensional gel electrophoresis of the proteins present in the $10\,000 \times g$ supernatant fraction corresponding to the lanes 2–4 in 6A (top panel), and pellet fraction corresponding to the lane 1 in 6A (bottom panel). After separation, the gel was blotted onto a nitrocellulose membrane and probed with mAb K37-142-1. (C), (D) Analysis of tyrosine phosphorylation of the crn7 protein. The protein was immunoprecipitated from the $10\,000 \times g$ pellet (lane 1) and supernatant (lane 2) using mAb K37-142-1. After separation, the gel was blotted onto the nitrocellulose membrane and probed with anti-phosphotyrosine (C) or anti-crn7 (D) antibody. (E), (F) Solubilization of the membrane compartments from the $10\,000 \times g$ pellet with Triton X-100. The $10\,000 \times g$ pellet was resuspended in homogenization buffer [6] and separated into two aliquots. One aliquot was treated with 0.5% Triton X-100 for 30 min at 4 °C, the other one served as control. Both aliquots were centrifuged again and the pellets and supernatants analyzed by Western blot. Lane 1 shows the $10\,000 \times g$ pellet; lane 2, the supernatant. E, control pellet; F, Triton X-100-treated pellet. Top panels, Western blot with anti-crn7 antibody; bottom panels, with anti-β-actin antibody.

labeled transferring and do not show any Rab5 or LIMP-1 staining (data not shown). We assume that these structures may be the Golgi/ER export vesicles. Another possibility is that they represent large protein complexes constituting the cytosolic pool of the crn7 protein.

To further confirm our results concerning the subcellular localization of crn7, we performed differential centrifugation experiments. The protein is unequally distributed between the cytosol and membrane fractions, the bulk of it being found in the cytosol (Fig. 7A), where it is present in a free state ($200\,000 \times g$ supernatant) as well as in large protein complexes ($200\,000 \times g$ pellet). The membrane-associated crn7 protein can be extracted from the $10\,000 \times g$ fraction upon treatment with Triton X-100 (Fig. 7E and F, upper panels). As a control, we used anti-β-actin antibody (Fig. 7E and F, lower panels), showing that only the detergent-sensitive membrane components have been extracted, but not cytoskeletal elements.

Separation of the post-nuclear supernatant on the discontinuous sucrose gradient has revealed that the protein fractionates in two sharp peaks corresponding to approx. 10–15% and 40–50% of sucrose, thus indicating the presence of the protein in light (vesicles) and heavy (Golgi) membrane compartments, respectively (data not shown).

3.4. *Properties of cytosolic and membrane-associated forms of crn7*

We also analyzed the crn7 protein in membrane and cytosolic fractions by means of 2D gel electrophoresis. Our results evidence that the pI values of the cytosolic form of the protein range between 5.2 and 6.0 with a peak corresponding to the predicted value of 5.6, whereas the membrane-associated form has pI values ranging from 4.5 to 6.0 (Fig. 7B), inferring that the membrane bound form is phosphorylated. Furthermore, when we immunoprecipitated crn7 from the cytosol and membrane fractions ($10\,000 \times g$ pellet) using mAb K37-142-1 coupled to protein G-sepharose beads in the presence of phosphatase inhibitors, the precipitated protein specifically reacted with an anti-tyrosine antibody. No labeling was observed with phosphoserine/threonine specific antibodies (data not shown). Moreover, our results indeed confirm that it is the membrane-associated, but not cytosolic form of crn7 which is phosphorylated on tyrosine residue(s) (Fig. 7C). There are several conserved tyrosines in the protein sequence that might be the targets for phosphorylation. Y738 is conserved among both crn7, POD-1, Dpod-1 and mammalian coronins 2A and 3, Y712 is conserved in crn7, and both POD-1 proteins. Several other tyrosine residues are present in crn7 and one or several coronins or POD-1 proteins.

4. Discussion

In the present study we characterize crn7, a novel ubiquitous mammalian protein. In contrast to the other coronin family members, it possesses two coronin domains, each consisting of several tandem WD repeats. Another remarkable feature of crn7 is a short serine-, proline- and threonine-rich low complexity region immediately C-terminal to the second coronin domain.

According to our results, crn7 is present as early as at the day 5 of mouse embryonic development in the majority of tissues and is upregulated in brain and thymus in the course of development. The data on tissue distribution of the protein imply that the protein is involved in cell differentiation events, involving the establishment of cell polarity. For example, crn7

is strongly expressed in the anterior-most parts of the lens cells in the developing eye, as well as in apical layers of the epidermis, in differentiated intestinal epithelium cells and in several subsets of brain neurons. All these cells do indeed change their morphology as they differentiate, the changes including polarization and development of cell extensions.

As we demonstrate here, crn7 is present in the cytosol and to the lesser extent on vesicles and at the Golgi. Since, according to sequence analysis, the protein lacks both transmembrane domains and signal peptides, we assume that it is rather localized to the cytoplasmic side of the Golgi membrane than to the luminal side or the lumen itself. Furthermore, our data clearly evidence that the detergent-sensitive membrane-associated pool of crn7 protein is phosphorylated on tyrosine, while the cytosolic one is not. Thus, phosphorylation may act as a signal controlling the membrane localization of crn7 protein. Importantly, crn7 does not bind F-actin, which is in a stark contrast to the other coronins and POD-1 proteins.

Several conventional coronins are also localized to the intermediates of the intracellular membrane trafficking pathways [11,18]. Taking into consideration the fact that crn7 does not co-localize with actin in any of the cells studied, we suggest that its WD repeats play a role different from actin binding. In this context it is particularly interesting that, apart from actin-binding proteins (such as Arp2/3 complex subunits or AIP1), two of the coatomer proteins participating in Golgi-related vesicular trafficking, namely α- and β′-COP, also possess several N-terminal WD repeats each. Furthermore, rabconnectin 3, an adaptor protein scaffolding both GDP/GTP exchange protein and GTPase-activating protein for Rab3 on synaptic vesicles, is predicted to have 12 WD domains [19]. Taken together, these data imply that crn7 and other multi-WD40 domain proteins may act as localized platforms for clustering either cargo, coatomer or regulatory molecules on the intracellular membranes and thus regulate the trafficking. Crn7 protein may function in this way by being translocated from the cytosol to the specific domains of the Golgi membrane upon tyrosine phosphorylation. As it was established previously, tyrosine phosphorylation does indeed act as a signal to recruit a variety of proteins to the membranes [20,21].

Other POD-1 proteins may also participate in the intracellular trafficking events. Indeed, the properties of the worm protein indicate that its function is related to the membrane transport. For instance, the eggshell defect of the POD-1 mutant worm embryos [13] implies that the protein is required for the correct secretion. Also, mislocalization of the polar granules and accumulation of abnormal membrane structures in the mutant embryos strongly indicate that POD-1 is needed for targeting the intracellular vesicles to the appropriate locations. On the other side, in *Dpod1* mutant fly embryos, the axons in the developing nervous system exhibit guidance defects; neuronal overexpression of *Dpod1* is also sufficient to disrupt the guidance. Furthermore, overexpression of the Dpod-1 protein in S2 cells causes them to form neurite-like actin-enriched processes [14]. Noteworthy, the *Drosophila* homologue seems to be at least partially localized to the perinuclear actin-unrelated compartment and to cytosolic vesicle-like structures in S2 cells, although the authors do not discuss this finding [14]. To summarize, both fly and worm proteins clearly demonstrate cell polarity-related functions and probably execute those by regulating membrane trafficking. Our data are thus in good agreement with those available for other unconventional coronins. It is however noteworthy that both POD-1 and Dpod-1 bind to F-actin, whereas crn7 does not. Two arising possibilities are that either crn7 interacts with the cytoskeletal elements via adaptor proteins, or it functions in cytoskeleton-independent manner.

To summarize, we propose a role for crn7 in the developmental events involving the ER-to-Golgi trafficking and resulting in establishment of polarity in cells and embryos. Further studies will be required to unravel the function of crn7 at the molecular level.

Acknowledgements: The work is supported by the Imhoff Stiftung and the Fonds der Chemischen Industrie. V.R. is a recipient of a PhD fellowship from the Graduate School in Genetics and Functional Genomics at Cologne University. We thank the MRC Center for the EST clones and Drs. Mark McNiven (Rochester, MN) and Yoshitaka Tanaka (Fukuoka) for sharing reagents. V.C. Padmakumar is acknowledged for technical help, Dr. Francisco Rivero for helpful suggestions on the phylogenetic analysis, Dr. Iakowos Karakesisoglou and Thorsten Libotte for critically reading the manuscript.

References

[1] de Hostos, E.L. (1999) Trends Cell Biol. 9, 345–350.
[2] de Hostos, E.L., Rehfuess, C., Bradtke, B., Waddell, D.R., Albrecht, R., Murphy, J. and Gerisch, G. (1993) J. Cell Biol. 120, 163–173.
[3] Maniak, M., Rauchenberger, R., Albrecht, R., Murphy, J. and Gerisch, G. (1995) Cell 83, 915–924.
[4] Hacker, U., Albrecht, R. and Maniak, M. (1997) J. Cell Sci. 110, 105–112.
[5] Asano, S., Mishima, M. and Nishida, E. (2001) Genes Cells 6, 225–235.
[6] Spoerl, Z., Stumpf, M., Noegel, A.A. and Hasse, A. (2002) J. Biol. Chem. 277, 48858–48867.
[7] Goode, B.L., Wong, J.J., Butty, A.-C., Peter, M., McCormack, A.L., Yates, J.R., Drubin, D.G. and Barnes, G. (1999) J. Cell Biol. 144, 83–89.
[8] Oku, T., Itoh, S., Okano, M., Suzuki, A., Suzuki, K., Nakajin, S., Tsuji, T., Nauseef, W.M. and Toyoshima, S. (2003) Biol. Pharm. Bull. 26, 409–416.
[9] Humphries, C.L., Balcer, H.I., D'Agostino, J.L., Winsor, B., Drubin, D.G., Barnes, G., Andrews, B.J. and Goode, B.L. (2002) J. Cell Biol. 159, 993–1004.
[10] Heil-Chapdelaine, R.A., Tran, N.K. and Cooper, J.A. (1998) Curr. Biol. 8, 1281–1284.
[11] Itoh, S., Suzuki, K., Nishihata, J., Iwasa, M., Oku, T., Nakajin, S., Nauseef, W.M. and Toyoshima, S. (2002) Biol. Pharm. Bull. 25, 837–844.
[12] Suzuki, K., Nishihata, J., Arai, Y., Honma, N., Yamamoto, K., Irimura, T. and Toyoshima, S. (1995) FEBS Lett. 364, 283–288.
[13] Rappleye, C.A., Paredez, A.R., Smoth, C.W., McDonald, K.L. and Aroian, R.V. (1999) Genes Dev. 13, 2838–2851.
[14] Rothenberg, M.E., Rogers, S.L., Vale, R.D., Jan, L.Y. and Jan, Y.-N. (2003) Neuron 39, 779–791.
[15] Okumura, M., Kung, C., Wong, S., Rodgers, M. and Thomas, M.L. (1998) DNA Cell Biol. 17, 779–787.
[16] Majoul, I., Sohn, K., Wieland, F.T., Pepperkok, R., Pizza, M., Hillemann, J. and Söling, H.D. (1998) J. Cell Biol. 143, 601–612.
[17] Thyberg, J. and Moskalewski, S. (1999) Exp. Cell Res. 246, 263–279.
[18] Rauchenberger, R., Hacker, U., Murphy, J., Niewohner, J. and Maniak, M. (1997) Curr. Biol. 7, 215–218.
[19] Nagano, F., Kawabe, H., Nakanishi, H., Shinohara, M., Deguchi-Tawarada, M., Takeuchi, M., Sasaki, T. and Takai, Y. (2002) J. Biol. Chem. 277, 9629–9632.
[20] Fingerhut, A., von Figura, K. and Höning, S. (2001) J. Biol. Chem. 276, 5476–5482.
[21] Cha, H. and Shapiro, P. (2001) J. Cell Biol. 153, 1355–1367.
[22] Pawson, T. (2004) Cell 116, 191–203.